Stereoselective Hydrogenation

International Edition: DOI: 10.1002/anie.201600345
German Edition: DOI: 10.1002/ange.201600345

Single-Face/All-*cis* Arene Hydrogenation by a Supported Single-Site d^0 Organozirconium Catalyst

Madelyn Marie Stalzer, Christopher P. Nicholas, Alak Bhattacharyya, Alessandro Motta, Massimiliano Delferro, and Tobin J. Marks**

Abstract: *The single-site supported organozirconium catalyst Cp*ZrBz$_2$/ZrS (Cp* = Me$_5$C$_5$, Bz = benzyl, ZrS = sulfated zirconia) catalyzes the single-face/all-cis hydrogenation of a large series of alkylated and fused arene derivatives to the corresponding all-cis-cyclohexanes. Kinetic/mechanistic and DFT analysis argue that stereoselection involves rapid, sequential H_2 delivery to a single catalyst-bound arene face, versus any competing intramolecular arene π-face interchange.*

The stereo-controlled hydrogenation of substituted aromatic molecules is of great interest for pharmaceutical, agrochemical, and fine chemical applications, where the required function is ultimately determined by the molecular stereochemistry.[1] Of particular interest for many applications is the selective creation of more saturated product stereoisomers, however these can be difficult to purify. Alkyl-substituted arenes such as xylenes have been the subject of extensive studies, as building blocks for more complex systems. Investigations with conventional heterogeneous hydrogenation catalysts such as Ni, Rh, Ru, Pt, and Pd have explored the scope and mechanism of both liquid phase and vapor-phase transformations.[2] Several studies reported promising selectivities (> 90 %) for the thermodynamically less favored *cis*-cyclohexanes, however these catalysts require harsh reaction conditions (> 50 bar H_2, > 50 °C, acid solvents).[3] To date, an allylcobalt system is a rare example of a homogenous arene hydrogenation catalyst with excellent *cis* selectivity (> 95 %), however it undergoes rapid deactivation with < 15 % conversions achieved.[4] Stereospecific syntheses of simple cyclic alkanes would provide new synthetic precursors for a variety of value-added products. This objective is timely since the great recent advances in selective alkane activation have provided many new transformations applicable to stereopure saturated hydrocarbons,[5] as illustrated by those for *cis*-dimethylcyclohexane (Scheme 1). Owing to the versatility of alcohols and ketones as synthetic intermediates, these products can then be modified in many ways to afford a variety of valuable substances.[5–8]

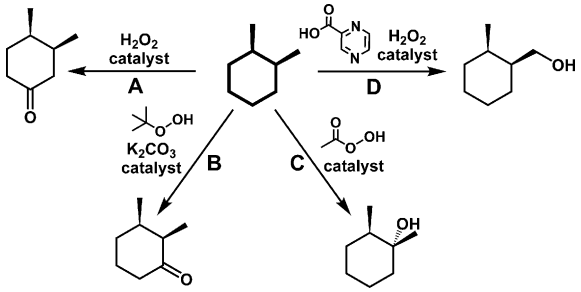

Scheme 1. Representative syntheses of versatile intermediates from *cis*-dimethylcyclohexane. A) Catalyst: Fe^{II}-DCBPY, DCBY = 2,2′-bipyridine-4,4′-dicarboxylic acid.[6] B) Catalyst: hypervalent iodine reagent.[7] C) Stereospecific catalyst: LMn(O)$_3$MnL^{2+}(PF$_6^-$)$_2$, L = 1,4,7-trimethyl-1,4,7-triaza-cyclononane.[8] D) Catalyst: {VO(OEt)(EtOH)}$_2$L, H$_4$L = bis(2-hydroxybenzylidene)-terephthalohydrazide.[9]

Single-site, molecule-derived supported catalysts have attracted interest due to their hybrid character combining the complementary features of traditional hetero- and homogeneous systems.[10] In particular, electrophilic d^0 catalysts supported on "super" Brønsted acids with large percentages of catalytically significant sites (70 % −98 %) exhibit high activity in technologically relevant olefin polymerization and hydrogenation processes.[11] Our group recently reported the kinetics and reaction pathways by which benzene and toluene hydrogenation are catalyzed by Cp*ZrR$_3$ complexes (Cp* = η^5-C$_5$(CH$_3$)$_5$; R = Me,[12] CH$_2$Ph;[13] Figure 1 A) chemisorbed on Brønsted acidic sulfated oxides (Cp*ZrR$_2$/MS, M = Zr, Al). Characterization included combined experimental spectrosopic (solid state NMR and XAS) and computational (DFT) methods. The results indicate the surface organozirconium moieties have elongated Zr···O$_{AlS}$ distances of 2.35(2) Å, indicating largely electrostatic, non-directional, ion pairing between the d^0 organometallic electrophiles and the charge-delocalized oxide surface.

In the aforementioned study, benzene hydrogenation proceeds with very large turnover frequencies, 1200 (mol benzene)(mol Zr)$^{-1}$h^{-1} over Cp*ZrMe$_2$/ZrS and 800 (mol benzene)(mol Zr)$^{-1}$h^{-1} over Cp*ZrBz$_2$/ZrS),[13] with complete selectivity to cyclohexane, and no detectable partially hydrogenated products. Furthermore, C$_6$D$_6$ hydrogenation over Cp*ZrMe$_2$/ZrS (Figure 1 B) proceeds via pairwise H_2 addition to both arene faces, yielding only isotopomers ααα (all-*cis*) and αβα (*cis-trans-cis*) in a 1:3.1 ratio (Fig-

[*] M. M. Stalzer, Dr. M. Delferro, Prof. T. J. Marks
Department of Chemistry, Northwestern University
2145 Sheridan Rd., Evanston, IL 60608 (USA)
E-mail: m-delferro@northwestern.edu
t-marks@northwestern.edu
Dr. C. P. Nicholas, Dr. A. Bhattacharyya
Exploratory Catalysis Research, UOP LLC, a Honeywell Company
25 E. Algonquin Rd, Des Plaines, IL 60017 (USA)
Dr. A. Motta
Dipartimento di Chimica and INSTM UdR Roma, Universitá degli Studi di Roma "La Sapienza"
P.le A. Moro 5, 00185 Roma (Italy)

Supporting information for this article can be found under: http://dx.doi.org/10.1002/anie.201600345.

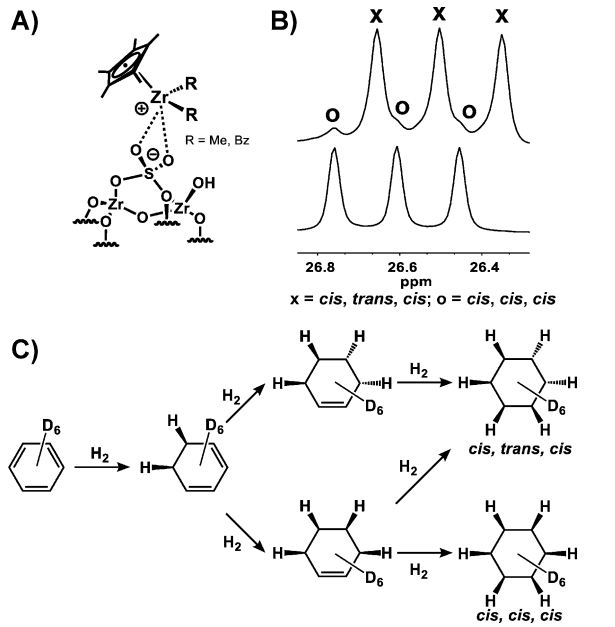

Figure 1. A) Schematic structure of chemisorbed Cp*ZrR_3 (R = Me, Bz) complexes on Brønsted acidic sulfated zirconia based on SS NMR, XAFS, and DFT data.[12] B) $^{13}C\{^1H\}$ spectra of the cyclohexane derived from Cp*$ZrMe_2$/ZrS (top) and Cp*$ZrBz_2$/ZrS (bottom) catalyzed hydrogenation of C_6D_6. Symbols *x* and o denote the two isotopomers. C) Pairwise addition scheme for the formation of two $C_6D_6H_6$ isotopomers. Deuterium atoms omitted for clarity.

ure 1 C).[14,15] In contrast, Cp*$ZrBz_2$/ZrS-mediated hydrogenation yields exclusively the all-*cis* isotopomer, consistent with kinetically negligible competing exchange of arene faces versus Cp*$ZrMe_2$/ZrS.[14a,16] Note that CPMAS ^{13}C NMR indicates that Cp*$ZrBz_2$/ZrS undergoes only partial Zr-benzyl hydrogenolysis to form a Cp*Zr(H)Bz/ZrS active species (see below), whereas Cp*$ZrMe_2$/ZrS undergoes complete Zr-CH_3 hydrogenolysis to form Cp*ZrH_2/ZrS.[13] The steric, electronic, and posssible π-stacking benzyl ligand characteristics of Cp*Zr(H)Bz/ZrS may create an environment which facilitates all-*cis* arene hydrogenation. These observations raise intriguing questions about the scope, selectivity, and systematics of this π-face H_2 delivery.

Here we report the single-face/all-*cis* hydrogenation of arene derivatives mediated by Cp*Zr(H)Bz/ZrS. Hydrogenation of a series of poly-alkylbenzenes and other fused arenes is shown to proceed solely at a single arene face under mild conditions, providing stereopure substituted cyclohexanes. Initial catalytic reactions were performed in pressure-rated glass reactors interfaced to a high vacuum line. In a typical run, a reactor was charged with 2.0 mL neat substrate dried over Na/K alloy and 50 mg of catalyst (2.4×10^{-6} mol of Zr), interfaced to the reaction line, evacuated to 10^{-5} Torr at −196 °C, warmed to 25 °C, and pressurized with 7 atm H_2. Reactions were carried out for 1 h with > 1450 rpm stirring which was shown to minimize mass transfer effects (see Table S5 in the Supporting Information), and the products were analyzed by ^1H NMR and GC-MS. Product stereoisomer assignments were made from known boiling points using DB-5 GC column separations with slow program ramp rates, and comparisons with the products of Pd/C-catalyzed hydrogenations (see Supporting Information for details). For *o*-xylene hydrogenation (Table 1, entry 1), a single product is observed, which, by comparison with commercially available dimethylcyclohexanes, is determined to be *cis*-1,2-dimethyl-cyclohexane (Figure 2 A and D). No partial hydrogenation products such as *o*-dimethylcyclohexadienes or *o*-dimethylcyclohexenes are detected, in agreement with the aforementioned benzene hydrogenation results.[12–14,17] Likewise, *m*- and *p*-xylene hydrogenated under identical conditions yield exclusively the respective *cis*-fully hydrogenated products (Table 1; Figure 2 B and E, C and F). Initial turnover frequencies (TOFs) fall in the order *o*-xylene > *m*-xylene > *p*-xylene.

Table 1: *Cis*-selective xylene hydrogenation.

Entry	Substrate[a]	Product	*Cis*-Selectivity [%]	Initial TOF[b]
1			> 99	1000
2[c]			> 99	880
3			> 99	470
4		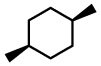	> 99	120

[a] Conditions: 2.0 mL substrate, 50 mg Cp*$ZrBz_2$/ZrS (2.4×10^{-6} mol of Zr), constant 7 atm H_2, 1 h, 25 °C, 1450 rpm. [b] TOF: (mol xylene) (mol Zr)$^{-1}$ h^{-1}. [c] Recycling experiment: after each cycle, all volatiles were vacuum-transferred from the catalytic reactor to a −78 °C container for further analysis. The supported catalyst was then dried under vacuum for 1 h before substrate addition for the 2nd cycle. For 3rd and 4th recycle experiments, see SI.

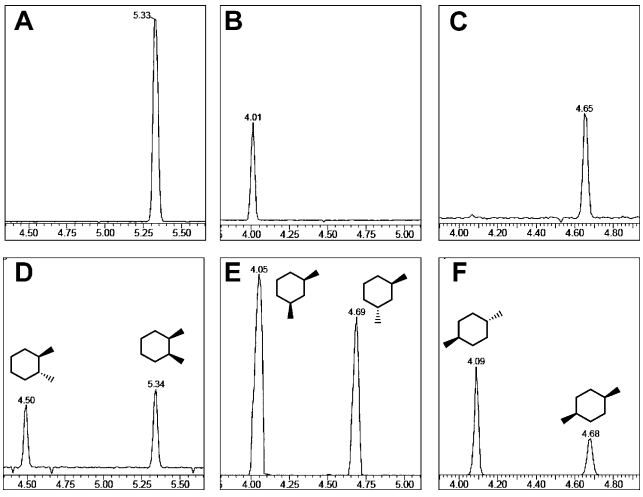

Figure 2. GC-MS chromatograms on a DB-5 column, 40–70 °C at 3 °C min^{-1}. A–C) Dimethylcyclohexane products from Cp*$ZrBz_2$/ZrS mediated xylenes hydrogenation. D–E) Dimethylcyclohexane products from Pd/C mediated hydrogenation. Substrates are as follows: A, D) *o*-xylene; B, E) *m*-xylene; C, F) *p*-xylene.

Catalyst temporal characteristics were next investigated in a series of three hydrogenation cycles with Cp*ZrBz$_2$/ZrS as the catalyst. After each cycle, all volatiles were vacuum-transferred from the reactor to a −78 °C trap for further analysis. The supported catalyst was then dried in vacuo for 1 h before substrate addition for the next cycle. For each cycle (for 2nd cycle data see Table 1, entry 2; for 3rd cycle data see Table S4), negligible variation in product *cis*-selectivity (>99%) is observed, suggesting that one benzyl group remains bound to the Zr^{IV} center. The decrease in *o*-xylene hydrogenation TOF[18] in succeeding cycles likely reflects small trace impurities.[13]

The structure of ^{13}C-enriched Cp*Zr(^{13}CH$_2$Ph)$_2$/ZrS was investigated by ^{13}C CPMAS NMR before and after *o*-xylene hydrogenations (Figure S13). The spectrum before catalytic runs shows four major resonances at $\delta = 128.0$, 125.0, 74.0, and 11.2 ppm, assigned, respectively to aromatic carbons, Zr-CH$_2$-*Ph*, Cp* framework, the ^{13}C-enriched Zr-^{13}*CH$_2$*-Ph group, and Cp*-Me carbon atoms. The downfield shifted broad signal at $\delta = 74.0$ ppm clearly indicates the formation of a "cation-like" electron-deficient organozirconium surface species as evidenced by comparison to model ion pair Zr(CH$_2$Ph)$_3^+$-B(CH$_2$Ph)(C$_6$F$_5$)$_3^-$ ($\delta = 74.8$ ppm)[19] versus neutrally charged Zr(CH$_2$Ph)$_3$[(CH$_3$C)CO] ($\delta =$ 65.7 ppm).[20] After exposure to reaction conditions (*o*-xylene, 1 atm H$_2$) for 1 hour, partial hydrogenolysis (40 ± 5%, Figure S13) of the ^{13}C-enriched Zr-CH$_2$-Ph moieties is observed, in accord with formation of catalytically active cationic Cp*Zr(H)Bz/ZrS.[21]

Kinetic analysis of Cp*ZrBz$_2$/ZrS-catalyzed *o*-xylene hydrogenation at 25 °C indicates a rate law first-order in [Zr], first-order in [H$_2$], and approximately zero-order in [*o*-xylene] over a broad range of arene concentrations.[22] Kinetic measurements on Table 1, entry 1 between 0 and 45 °C at constant 7 atm of H$_2$ with rapid (>1450 rpm) stirring to minimize mass transfer effects (Table S5) combined with a standard Eyring/Arrhenius analysis yields $\Delta H^{\ddagger} = 4.8 \pm 0.5$ kcal mol^{-1}, $\Delta S^{\ddagger} = -58.7 \pm 1.9$ eu, and $E_a = 5.3 \pm 0.6$ kcal mol^{-1}, suggesting a highly organized transition state (large negative $\Delta S^{\ddagger}$), typical of many d^0/f^n-centered catalytic processes,[23] and an intermolecular turnover-limiting step—the first H$_2$ delivery. The observed E_a (5.3 kcal mol^{-1}) is somewhat lower than those for conventional supported metal nanoparticle *o*-xylene hydrogenation catalysts ($E_a = 7.4$–14.9 kcal mol^{-1}).[24]

DFT modeling was next carried out to gain further insight into the remarkable *cis*-selectivity of the Cp*Zr(H)Bz/ZrS-catalyzed hydrogenation and the reaction kinetics.[13] The ZrS surface model consists of a 4 × 2 slab (12.85 × 14.50 × 30 Å) built starting from the (101) plane cut from the optimized bulk structure of tetragonal zirconia (See SI for more details).[25] The six layer surface was saturated with four dissociated pyrosulfuric acid and four undissociated water molecules [S$_2$O$_7^-$, 2H$^+$, H$_2$O]. The lowest oxygen layer was fixed during the geometry optimization to simulate bulk constraints. The most stable anionic surface was found by removing the most acidic hydrogen from the surface. Only one organozirconium cation was placed on the anionic surface to avoid lateral interactions. The Gibbs free energy profile

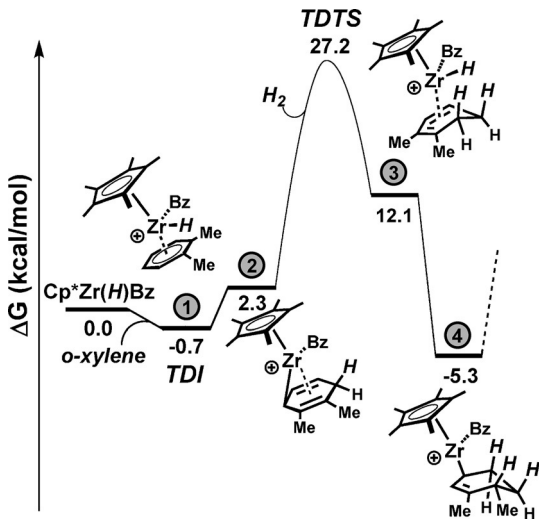

Figure 3. Energy profile (kcal mol^{-1}) of the first *o*-xylene hydrogenation subcycle at Cp*Zr(H)Bz/ZrS (see Figure S3 for the entire profile). The ZrS surface is omitted for clarity.

shown in Figure 3 indicates that *o*-xylene coordination (**1**) is slightly exergonic ($\Delta G = -0.7$ kcal mol^{-1}) and the first H-transfer step is barrierless, leading to slightly endergonic intermediate **2**. The energetic demands of the first H$_2$ addition primarily reflect the entropic contribution associated with the H$_2$ activation/binding. The subsequent Zr-C hydrogenolysis leads to dimethyl-hexadiene complex **3** that spontaneously evolves to stable intermediate **4** via a barrierless second H-transfer. The second and third H$_2$ additions occur in a similar manner, but lie at lower energies. An energetic span model[26] was next used to probe the energetic difference (Table S1) between the coordinated arene species (TOF determining intermediate, TDI) and the first Zr-C hydrogenolysis transition state (TOF determining transition state, TDTS). Note that xylene coordination lies outside the TDI and TDTS range and only one H$_2$ addition lies within the TDI—TDTS range, indicating a kinetic rate law zero-order in [xylene] and first-order in [H$_2$], in good agreement with experiment. The computed energetic barriers follow the trend *o*-xylene < *m*-xylene < *p*-xylene (27.9, 28.7, and 34.4 kcal mol^{-1}), respectively, again in good agreement with experiment (Tables 1 and S1). The relative TDI and TDTS stability found for the *o*- *m*- and *p*-xylenes reflects an interplay of steric and electronic effects.

Exclusive formation of all-*cis* isomers with Cp*Zr(H)Bz$_2$/ZrS but not with Cp*ZrH$_2$/ZrS (Figure 1) suggests that coordinated substrate π-face exchange is insignificant in the former on the catalytic timescale. Two arene face exchange pathways are conceivable: 1) Zr-substrate dissociation/re-coordination (note that that free dienes and olefins are not detected during the course of these reactions). 2) Face exchange within the Zr coordination sphere.[27] To probe the energetics of dissociation/re-coordination, DFT analysis focused on the dissociation energetics of xylene and olefinic intermediates present during the hydrogenation cycle for Cp*ZrH$_2$/ZrS versus Cp*Zr(H)Bz/ZrS. It is found that all species bind more strongly to Cp*ZrH$_2$/ZrS than to Cp*Zr-

Table 2: Computed Gibbs free energy (kcal mol^{-1}) of decomplexation for *o*-xylene, 1,2-dimethylcyclohexadiene, 1,2-dimethylcyclohexene, and 1,2-dimethylcyclohexane from Cp*ZrH_2/ZrS and Cp*Zr(H)Bz/ZrS.

	Cp*ZrH_2/ZrS	Cp*Zr(H)Bz/ZrS
o-xylene	25.1	0.7
1,2-dimethylcyclohexadiene	36.2	5.7
1,2-dimethylcyclohexene	11.0	4.5
1,2-dimethylcyclohexane	4.1	−1.8

(H)Bz/ZrS (Table 2), intuitively consistent with the more coordinatively unsaturated/-electrophilic character of Cp*ZrH_2/ZrS versus Cp*Zr-(H)Bz/ZrS, and in agreement with a Natural Bond Orbital (NBO) charge analysis of the Cp*ZrH_2^+ ($Zr^{+1.4}$) and Cp*Zr(H)Bz^+ ($Zr^{+1.1}$) naked cations. That only Cp*Zr(H)Bz displays complete facial selectivity argues that another pathway is operative. Substrate or bound diene face exchange may proceed intramolecularly, assisted by agostic interactions,[14a,28] which may be more stable/accessible at less encumbered/more electrophilic Cp*ZrH_2/ZrS. This possibility is currently under investigation.

The aromatic substrate scope was next explored under the aforementioned reaction conditions, and results are summarized in Table 3. Catalytic versatility is evidenced by high selectivity in di- and tri-substituted arene hydrogenation, along with naphthalene, and at reasonable TOFs. Stereoselection for tri-substituted arenes is particularly noteworthy because there has never, to our knowledge, been a source of stereopure *cis*-1,2,3-trimethylcyclohexane (entry 4), *cis*-1,3,5-trimethylcyclohexane (entry 5), or *cis*-1,2,4- trimethylcyclohexane (entry 6). Naphthalene hydrogenation is also notable in that intermediate tetralin is observed, in addition to fully hydrogenated *cis*-decalin (entry 7). That the tetralin TOF (40 h^{-1}, entry 8) is greater than that of naphthalene (10 h^{-1}) implies that tetralin is the initial naphthalene hydrogenation product and may be released from the catalyst, then undergoes hydrogenation to *cis*-decalin. Due to the electrophilic nature of these Zr species, this catalyst is sluggish or inactive in the presence of polar functional groups.

Table 3: Substrate scope for stereoselective arene hydrogenation.

Entry	Substrate[a]	Product	*Cis*-Selectivity [%]	Initial TOF[b]
1			>99	430
2			>99	40
3	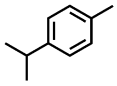	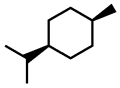	≈90[29]	110
4			>99	130
5		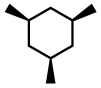	>99	70
6		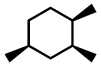	>99	20
7			>99	10
8			>99	40

[a] Conditions: 2 mL substrate, 50 mg Cp*$ZrBz_2$/ZrS (2.4×10^{-6} mol of Zr), constant 7 atm H_2, 1 h, 25 °C, ≥1450 rpm. [b] In (mol arene)(mol Zr)$^{-1}$ h^{-1}.

In summary, single-site supported Cp*Zr(H)Bz/ZrS mediates the highly face/*cis*-selective hydrogenation of substituted arenes to the corresponding *cis*-substituted cyclohexanes. The origin of this selectivity appears to reflect a balance between metal center properties which promote rapid, sequential H_2 delivery to the bound arene face, versus competing electrophilicity factors which enable intramolecular substrate π-face interchange. For xylenes, reaction rates fall in the order, *o*-xylene > *m*-xylene > *p*-xylene, doubtless reflecting steric and electronic effects that govern the turnover-limiting first H_2 addition step. Further studies are underway to explore additional reaction scope.

Experimental Section

A 75 mL pressure-rated glass reaction vessel with a Teflon screw top lid equipped with a quarter-turn plug was dried under high vacuum (5×10^{-7} Torr) for >1 h prior to experiments. In a glovebox the vessel was then charged with 50 mg of supported catalyst and 2.0 mL substrate, dried over Na/K. The sealed vessel was then transferred to a high vacuum line, evacuated at −196 °C, warmed to 25 °C, and filled with H_2 (7.0 atm). The mixture was then stirred rapidly (>1450 rpm) with a large stir bar at 25 °C for 1 h. The product was then analyzed by GC/MS and ^{1}H NMR. For detailed stereoisomer assignments see SI.

Acknowledgements

Financial support provided by UOP LLC, a Honeywell Company (Des Plaines, IL) and the Division of Chemical Sciences, Office of Basic Energy Sciences, Office of Energy Research, US Department of Energy (Grant DE-FG02-86ER13511). Purchases of NMR and GC-TOF instrumentation at the Integrated Molecular Structure Education and Research Center (IMSERC) of Northwestern Univ. were supported by NSF grants CHE-1048773 and CHE-0923236, respectively. Computational resources were provided by the Northwestern Univ. Quest High Performance Computing cluster (M.D.) and CINECA award HP10CBHAYD 2014 under the ISCRA initiative (A.M.). We thank Dr. J. C. Bricker of UOP for helpful discussions. A patent application partially based on this work has been filed (US Patent Application 14/559,380 2014).

Keywords: DFT calculations · organozirconium catalyst · stereoselective hydrogenation · sulfated oxides · supported catalysts

How to cite: *Angew. Chem. Int. Ed.* **2016**, *55*, 5263–5267
Angew. Chem. **2016**, *128*, 5349–5353

[1] K. W. Quasdorf, L. E. Overman, *Nature* **2014**, *516*, 181–191.
[2] a) T. Bera, J. W. Thybaut, G. B. Marin, *ACS Catal.* **2012**, *2*, 1305–1318; b) A. Kalantar Neyestanaki, P. Mäki-Arvela, H. Backman, H. Karhu, T. Salmi, J. Väyrynen, D. Y. Murzin, *J. Catal.* **2003**, *218*, 267–279; c) S. Toppinen, T. K. Rantakylä, T. Salmi, J. Aittamaa, *Ind. Eng. Chem. Res.* **1996**, *35*, 4424–4433.
[3] a) C. H. Pélisson, C. Hubert, A. Denicourt-Nowicki, A. Roucoux, *Top. Catal.* **2013**, *56*, 1220–1227; b) B. A. Kakade, S. Sahoo, S. B. Halligudi, V. K. Pillai, *J. Phys. Chem. C* **2008**, *112*, 13317–13319; c) J.-F. Sauvage, R. H. Baker, A. S. Hussey, *J. Am. Chem. Soc.* **1961**, *83*, 3874–3877.
[4] a) E. L. Muetterties, J. R. Bleeke, *Acc. Chem. Res.* **1979**, *12*, 324–331; b) L. S. Stuhl, M. Rakowski DuBois, F. J. Hirsekorn, J. R. Bleeke, A. E. Stevens, E. L. Muetterties, *J. Am. Chem. Soc.* **1978**, *100*, 2405–2410.
[5] a) J. Serrano-Plana, W. N. Oloo, L. Acosta-Rueda, K. K. Meier, B. Verdejo, E. García-España, M. G. Basallote, E. Münck, L. Que, A. Company, M. Costas, *J. Am. Chem. Soc.* **2015**, *137*, 15833–15842; b) A. K. Chattopadhyay, S. Hanessian, *Chem. Commun.* **2015**, *51*, 16437–16449; c) A. K. Chattopadhyay, S. Hanessian, *Chem. Commun.* **2015**, *51*, 16450–16467; d) P. L. Arnold, M. W. McMullon, J. Rieb, F. E. Kuehn, *Angew. Chem. Int. Ed.* **2015**, *54*, 82–100; *Angew. Chem.* **2015**, *127*, 84–103; e) M. Sun, J. Zhang, P. Putaj, V. Caps, F. Lefebvre, J. Pelletier, J.-M. Basset, *Chem. Rev.* **2014**, *114*, 981–1019; f) E. P. Talsi, K. P. Bryliakov, *Coord. Chem. Rev.* **2012**, *256*, 1418–1434; g) G. B. Shulpin, *Org. Biomol. Chem.* **2010**, *8*, 4217–4228; h) M. Lersch, M. Tilset, *Chem. Rev.* **2005**, *105*, 2471–2526; i) J. A. Labinger, *J. Mol. Catal. A* **2004**, *220*, 27–35.
[6] S. Cheng, J. Li, X. Yu, C. Chen, H. Ji, W. Ma, J. Zhao, *New J. Chem.* **2013**, *37*, 3267–3273.
[7] S. A. Moteki, A. Usui, T. Zhang, C. R. Solorio Alvarado, K. Maruoka, *Angew. Chem. Int. Ed.* **2013**, *52*, 8657–8660; *Angew. Chem.* **2013**, *125*, 8819–8822.
[8] J. R. Lindsay Smith, G. B. Shulpin, *Tetrahedron Lett.* **1998**, *39*, 4909–4912.
[9] M. Sutradhar, N. V. Shvydkiy, M. F. C. Guedes da Silva, M. V. Kirillova, Y. N. Kozlov, A. J. L. Pombeiro, G. B. Shulpin, *Dalton Trans.* **2013**, *42*, 11791–11803.
[10] a) C. Coperet, A. Comas-Vives, M. P. Conley, D. P. Estes, A. Fedorov, V. Mougel, H. Nagae, F. Nunez-Zarur, P. A. Zhizhko, *Chem. Rev.* **2016**, *116*, 323–421; b) R. C. Klet, S. Tussupbayev, J. Borycz, J. R. Gallagher, M. M. Stalzer, J. T. Miller, L. Gagliardi, J. T. Hupp, T. J. Marks, C. J. Cramer, M. Delferro, O. K. Farha, *J. Am. Chem. Soc.* **2015**, *137*, 15680–15683; c) M. P. Conley, C. Coperet, *Top. Catal.* **2014**, *57*, 843–851; d) C. Coperet, *Chem. Rev.* **2010**, *110*, 656–680; e) C. Copéret, M. Chabanas, R. Petroff Saint-Arroman, J.-M. Basset, *Angew. Chem. Int. Ed.* **2003**, *42*, 156–181; *Angew. Chem.* **2003**, *115*, 164–191; f) T. J. Marks, *Acc. Chem. Res.* **1992**, *25*, 57–65.
[11] M. M. Stalzer, M. Delferro, T. J. Marks, *Catal. Lett.* **2015**, *145*, 3–14.
[12] L. A. Williams, N. Guo, A. Motta, M. Delferro, I. L. Fragala, J. T. Miller, T. J. Marks, *Proc. Natl. Acad. Sci. USA* **2013**, *110*, 413–418.
[13] W. Gu, M. M. Stalzer, C. P. Nicholas, A. Bhattacharyya, A. Motta, J. R. Gallagher, G. Zhang, J. T. Miller, T. Kobayashi, M. Pruski, M. Delferro, T. J. Marks, *J. Am. Chem. Soc.* **2015**, *137*, 6770–6780.
[14] a) H. Ahn, C. P. Nicholas, T. J. Marks, *Organometallics* **2002**, *21*, 1788–1806; b) M. S. Eisen, T. J. Marks, *J. Mol. Catal.* **1994**, *86*, 23–50.
[15] For a system adhering to statistical thermodynamics, a ratio of 1:3 would be expected for the two isomers.
[16] a) L. Foppa, J. Dupont, *Chem. Soc. Rev.* **2015**, *44*, 1886–1897; b) A. Gual, C. Godard, S. Castillon, C. Claver, *Dalton Trans.* **2010**, *39*, 11499–11512; c) P. J. Dyson, *Dalton Trans.* **2003**, 2964–2974.
[17] a) C. P. Nicholas, T. J. Marks, *Nano Lett.* **2004**, *4*, 1557–1559; b) C. P. Nicholas, T. J. Marks, *Langmuir* **2004**, *20*, 9456–9462; c) C. P. Nicholas, H. S. Ahn, T. J. Marks, *J. Am. Chem. Soc.* **2003**, *125*, 4325–4331.
[18] In the third cycle, the *o*-xylene hydrogenation TOF is 60 (mol toluene)(mol Zr)$^{-1}$h^{-1} (Table S4), and the *cis*-stereroselectivity is $>99\,\%$.
[19] C. Pellecchia, A. Grassi, A. Immirzi, *J. Am. Chem. Soc.* **1993**, *115*, 1160–1162.
[20] T. V. Lubben, P. T. Wolczanski, G. D. Van Duyne, *Organometallics* **1984**, *3*, 977–983.
[21] Complete Zr-Bz hydrogenolysis to form Cp*ZrH_2/ZrS cannot be ruled out on the basis of the NMR data, but it is inconsistent with the exclusive single-face/all-*cis* arene hydrogenation stereochemistry (see Ref. [14]).
[22] These findings parallel the behavior of Cp*Zr(H)R(benzene)$^+$/ZrS^- benzene hydrogenation catalysts (R = H, Bz), with turnover-limiting first H_2 delivery to substrate.
[23] a) N. G. Stahl, M. R. Salata, T. J. Marks, *J. Am. Chem. Soc.* **2005**, *127*, 10898–10909; b) C. L. Beswick, T. J. Marks, *J. Am. Chem. Soc.* **2000**, *122*, 10358–10370.
[24] a) M. H. G. Prechtl, M. Scariot, J. D. Scholten, G. Machado, S. R. Teixeira, J. Dupont, *Inorg. Chem.* **2008**, *47*, 8995–9001; b) T. C. Ho, *Energy Fuels* **1994**, *8*, 1149–1151; c) M. V. Rahaman, M. A. Vannice, *J. Catal.* **1991**, *127*, 267–275.
[25] X. Li, K. Nagaoka, L. J. Simon, R. Olindo, J. A. Lercher, A. Hofmann, J. Sauer, *J. Am. Chem. Soc.* **2005**, *127*, 16159–16166.
[26] a) A. S. Dudnik, V. L. Weidner, A. Motta, M. Delferro, T. J. Marks, *Nat. Chem.* **2014**, *6*, 1100–1107; b) S. Kozuch, S. Shaik, *Acc. Chem. Res.* **2010**, *44*, 101–110.
[27] a) O. Kuehl, *Chem. Soc. Rev.* **2011**, *40*, 1235–1246; b) M. Brookhart, M. L. H. Green, G. Parkin, *Proc. Natl. Acad. Sci. USA* **2007**, *104*, 6908–6914; c) W. Scherer, G. S. McGrady, *Angew. Chem. Int. Ed.* **2004**, *43*, 1782–1806; *Angew. Chem.* **2004**, *116*, 1816–1842.
[28] a) G. J. Pindado, M. Thornton-Pett, M. Bochmann, *J. Chem. Soc. Dalton Trans.* **1997**, 3115–3127; b) H. Yasuda, Y. Kajihara, K. Mashima, K. Nagasuna, K. Lee, A. Nakamura, *Organometallics* **1982**, *1*, 388–396.
[29] The presence of $<10\,\%$ of *trans* isomer is probably due to steric factors which allow ring π-face interchange.

Received: January 12, 2016
Published online: March 17, 2016

